STREAMWISE VORTICES FOR TURBULENT BOUNDARY LAYER SEPARATION CONTROL

Angele Kristian Patrik
Department of Mechanics, KTH
S-100 44 Stockholm, Sweden
kristian@mech.kth.se

ABSTRACT

Streamwise vortices were employed to control a separating adverse pressure gradient turbulent boundary layer. Initially non-equidistant vortices become and remain equidistant and are confined to the boundary layer. The crucial parameter for successful backflow elimination is the amount of circulation introduced and the exact streamwise vortex generator position is only of indirect importance. This is an effect of the conserved circulation and the confined vortices. The vortices change the mean velocity profile and the asymptotic state is an S-shaped two-dimensional boundary layer determined by the vortex generator height.

INTRODUCTION

Turbulent boundary layer separation cause a severe reduction of performance in many technical applications and its control is thereby motivated. Passive control using different mixing devices for example vortex generators (VGs) is the traditional technique, see Schubauer and Spangenberger (1960). More recent investigations use miniature VGs with focus on minimizing the drag, see Lin *et al* (1989). The present work is a continuation of the investigation by Angele and Grewe (2002), where the velocity measurements were focusing on the near-field downstream of the VGs in a separating adverse pressure gradient tubulent boundary layer. In the present case the focus is on the effect on the separation bubble.

METHOD

Experimental setup

The experiments were carried out at KTH in a new closed loop wind-tunnel. The test section is 4.0 m long and has a cross-section area of 0.75 m×0.5 m (z and y-directions respectively). Most parts are made of Plexiglass to allow for the use of optical measurement techniques. The test section is interchangable and for the present experiments a special test section was designed. Figure 1 (a) shows a schematic picture of the test section. The first part has a constant cross-section area. At x=1.25 m the test section is diverged by means of a flexible wall (allowing a free choice of the wall shape) in order to achieve a decelerating flow. Suction is applied through holes in the curved wall in order to prevent the boundary layer from separating there. 1300 holes with a diameter of 5 mm were connected to four suction boxes between x=1.25 m and x=2.25 m, see the dashed lines in figure 1 (a). The suction boxes are connected via tubing to a 4.5 kW fan. The flow removal was estimated to be 6-7% of the total flow rate above the flat plate. A flat plate, vertically mounted in the test section, is exposed to an APG using this configuration. The flat plate consists of four 1.0 m long 20 mm thick Plexiglass segments. The first segment has a 0.2 m long symmetric super-elliptic leading edge. To be able to control and assure a non-separated leading edge flow, the last 0.5 m of the last plate segment was used as a flap. To trigger a spanwise homogeneous transition the boundary layer was tripped using a 0.4 mm zig-zag tape. The trip is placed 0.25 m downstream (Re_x=4.4·10^5) of the tip of the leading edge. This arrangement assured a fully developed turbulent ZPG boundary layer as initial condition well upstream of the expanding part of the test section. The flat plate is equipped with 48 pressure taps evenly distributed in downstream direction at every 0.1 m after the first meter. Pressure taps are also placed in the spanwise direction 0.175 m off the centerline at every second tap position after the first meter to check the spanwise homogeneity. The free-stream velocity at the inlet of the test section was $U_{inl.}$=26.5 m/s and the temperature was kept constant at 20°C using a cooling system.

PIV equipment

PIV measurements were conducted with an equipment consisting of a 400 mJ double pulsed Nd:Yag laser and a digital Kodak ES1.0 CCD camera, containing 1018 x 1008 pixels. The measurement process was synchronized and controlled by a hard- and software from Dantec. Between 200 and 1300 image pairs were used for calculating turbulence statistics. The spatial resolution, using image sizes of 150 mm × 150 mm and 32 × 32 pixel interrogation areas (ia), was 4.84 mm × 4.84 mm respectively. An overlap of 50% of the ia was used together with a Gaussian window function to minimize the loss-of-pairs. The time difference between the two image pairs was optimized based on the maximum excepted velocity in the streamwise direction being around Δt=60 μs in all the measurements. A maximum displacement of 25% of the ia is used together with a Peak Value Ratio (PVR) $\geq$1.2. This is sufficient for accurate mean values which can be used for a second validation, only accepting instantaneous values which are bounded by the mean values ± 3 rms in the both components. This criterion greatly improves the quality of the Reynolds stresses. The validation rate in the data is 90-98 %. The PIV data presented are averaged over 5-10 ias.

The uncontrolled flow field

In figure 1 (b) the downstream development of the pressure coefficient

$$c_p = \frac{p - p_{ref}}{p_0 - p_{ref}} \qquad (1)$$

for the wall-static pressure p and its gradient in this direction $\frac{\partial c_p}{\partial x}$ is shown. The reference wall-static pressure, p_{ref}, is

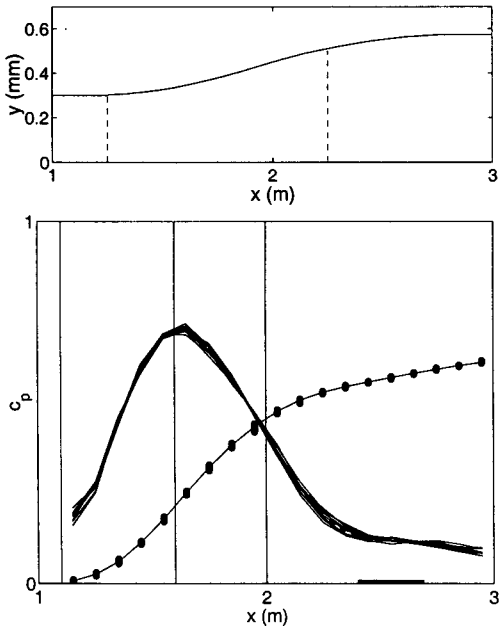

Figure 1: (a) Schematic view of the setup with suction applied on the curved surface between the vertical dashed lines. The uncontrolled case: (b) The wall static pressure distribution and its gradient. The horizontal full line shows the extent of the separated region and the vertical lines show the different positions of the VGs.

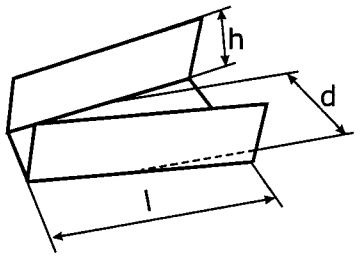

Figure 2: A VG creating a pair of counter-rotating streamwise vortices in downstream direction.

taken at x=0.45 m in the non-diverging part of the flow and p_0 is the stagnation pressure at this position. Using this setup creates a separating APG turbulent boundary layer with a weak and shallow separation bubble.

Streamwise vortices and measurement positions

The streamwise vortices introduced to control the separation bubble were generated by means of VGs. Figure 2 shows the geometry of a VG which creates a pair of counter-rotating vortices. l is the VG side length, h the height, d is the spanwise distance between two blades (at $l/2$) and D the spanwise distance between two VGs, see figure 4. Table 1 shows the design criteria used here as suggested by Pearcey (1961). The absolute value of the streamwise circulation introduced in the boundary layer is estimated as

$$\Gamma = \frac{Z}{D} hU \qquad U(H_{12,\Gamma=0}, U_\infty, h/\delta) \qquad (2)$$

where $Z = 750\ mm$ is the spanwise width of the flat

Table 1: VG design criteria suggested by Pearcey (1961). D is the spanwise distance between two VGs.

l/h	D/d	D/h
3	4	8.33

Table 2: Physical dimensions of the two different VG sets used.

h (mm)	d (mm)	l (mm)	D (mm)
18	37.5	54	150
30	62.5	90	250

Table 3: Different streamwise VG positions for varying the different parameters affecting Γ.

x_{VG} (m)	$H_{12,\Gamma=0}$	U_∞	h/δ	Γ
1.1	1.4	26.7	0.95	4.7
1.6	1.6	22.7	0.88	3.9
1.6	1.6	22.7	0.53	3.3
2.0	2.0	20.3	0.50	2.6

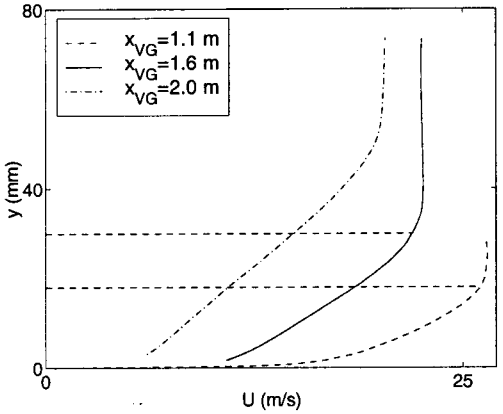

Figure 3: *The streamwise mean velocity profiles at the three different VG positions. The dashed lines corresponds to the VG heights h=18 mm and h=30 mm.*

plate and U the mean velocity at y=h. U is a function of the boundary layer characteristics where $H_{12,\Gamma=0}$ is the shape-factor, which reflects the effect of the pressure gradient on the shape of the boundary layer velocity profile, U_∞ is the local free-stream velocity and δ the local boundary layer thickness. By using two different VG sets, see table 2, at three different x-positions, see table 3 and figure 1 (b), $H_{12,\Gamma=0}$, U_∞ and h/δ could be varied and Γ changed. Figure 3 shows the uncontrolled streamwise mean velocity profiles at the three different downstream position where the VGs were positioned. The boundary layer thickness grows fast in downstream direction and the free-stream velocity is decreased as the pressure gradient acts on it. The profile is loosing its fullness, which is reflected in an increase of $H_{12,\Gamma=0}$.

Since VGs of different height are positioned at different streamwise positions, the vortices have different age, in terms of x/h, when considering a specific downstream position, see table 4.

PIV velocity and turbulence measurements are presented mainly for x=2.5 m which corresponds approximately to the position of the maximum backflow in the case with-

Table 4: Vortex age. Values within parenthesis are cases not measured.

Γ	$x = 2.5\ m$	$x = 3.4\ m$
4.7	x/h=78	x/h=128
3.9	(x/h=30)	x/h=60
3.3	x/h=50	(x/h=100)
2.6	x/h=17	(x/h=47)

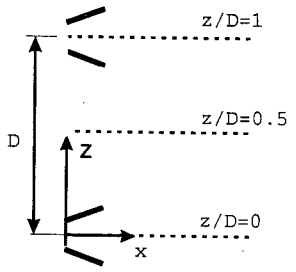

Figure 4: Two VGs and coordinate system seen from above. Flow is from left to right. PIV measurements were conducted covering the distance between two VGs at $z/D = 0$ and z/D=1.

out streamwise vortices (referred to as $\Gamma = 0$). Spanwise-downstream xz-planes, covering the distance between two VGs at $z/D = 0$ and z/D=1, see figure 4, were conducted at different wall-normal positions. Wall-normal measurements in the xy-plane were conducted at the different spanwise positions $z/D = 0$ and $z/D = 0.5$, see figure 4. xy-plane measurements were also made at x=3.4 m to investigate the asymptotic behavior of the vortices as well as xz-planes at the tip of the blade of a VG.

RESULTS: MEAN FLOW

Ability of backflow elimination

The streamwise vortices cause an inflow of high momentum fluid towards the wall region downstream of a VG. Between two vortices from two different VGs there is a region with common outflow towards the free-stream. The boundary layer thickness is varying in the spanwise direction as a consequence of this and the maximum boundary layer thickness occurs at the position of outflow, $\delta_{z/D=0.5}$. This is increasing with increasing circulation, see table 5, which is due to the fact that the outflow is enhanced as the circulation is increased.

Mean streamwise velocity profiles in the wall-normal direction at the position of outflow, are shown in figure 5 (a) for all the different amounts of circulation. The case without streamwise vortices shows a profile which is similar to a mixing layer. The case with the lowest amount of circulation Γ=2.6 does not change the mean velocity profile much at this position and its shape is very similar to the case without vortices which indicates that the backflow is not eliminated here. The behavior of the backflow coefficient in the spanwise direction is displayed in figure 5 (b) at $y = 10$ mm. This wall-normal position corresponds to different $y/\delta_{z/D=0.5}$ since $\delta_{z/D=0.5}$ is a function of the circulation. However, for all cases this corresponds to a wall-normal position of

Table 5: The effect of the streamwise vortices on the boundary layer parameters at the region of outflow.

Γ	$H_{12,z/D=0.5}$	$\delta_{z/D=0.5}$ (mm)
4.7	1.56	145
3.9	1.73	126
3.3	1.75	111
2.6	3.37	103.5
0	3.63	92

$y/\delta_{z/D=0.5} \leq 0.1$ *i.e.* below the local maximum in the mean velocity profile. For Γ=2.6 the backflow is not eliminated at all spanwise positions and a region of instantaneous backflow is formed with a maximum at the region of outflow. However, at the inflow positions right downstream of the VGs the backflow is near zero. The overall higher values of χ, which are approximately constant in the spanwise direction, corresponds to case without streamwise vortices. For $\Gamma \geq 3.3$ the backflow is eliminated at all spanwise positions and the shape of the velocity profile in the wall-normal direction, figure 5 (a), is drastically changed. The mean velocity profiles are S-shaped which is very different from the uncontrolled case. The shapefactor of the profile is an inverse function of the circulation, see table 5, and as the circulation is increased the shapefactor is decreased. This was also noted by Schubauer and Spangenberger (1960), however, this is not a good measure of the shape of these profiles. Figure 5 (c) shows variation of the streamwise mean velocity in the spanwise direction. A three-dimensional wake like structure is seen as opposed to the two-dimensional uncontrolled case and there is a stationary low velocity streak at the position of outflow. The case with the lowest circulation shows overall lower values of the streamwise velocity and at the position of outflow it is almost similar to the case without vortices which gives rise to the observed maximum in the backflow coefficient at this position.

Vortex generator height and streamwise position

Figure 5 (a) also shows the effect of using VGs of different relative height h/δ which introduce vortices of different size. The cases using $h/\delta \approx 1$ show vortices of approximately same relative size whereas the case with the smaller VG $h/\delta \approx 0.5$ shows a smaller S-shaped profile which means that the vortex center position is closer to the wall *i.e* the vortex is smaller. However, the size of the vortices do not seem to be of major importance at least not for relatively large vortices as the ones present here. The region which is important for backflow elimination is the near-wall region and not the outer region. One should also note that despite the fact that the cases are introduced at positions which correspond to widely different local pressure gradients, see figure 1 (b), they show similar profiles.

Equidistant vortices

The vortices are not equidistant initially since D/d=4. Considering the spanwise mean velocity component, see figure 6 (a), it can be seen that the vortices have all reached an equidistant state with maxima at z/D=0.25 and 0.75 which correspond to the vortex center positions. The reason for the backflow for the case of Γ=2.6 can not be blamed on the vortices not yet being equidistant which could lead to pockets of backflow. The probable explanation is that the circulation is not sufficient to completely eliminate the backflow along the whole spanwise direction. The vortices are equidistant

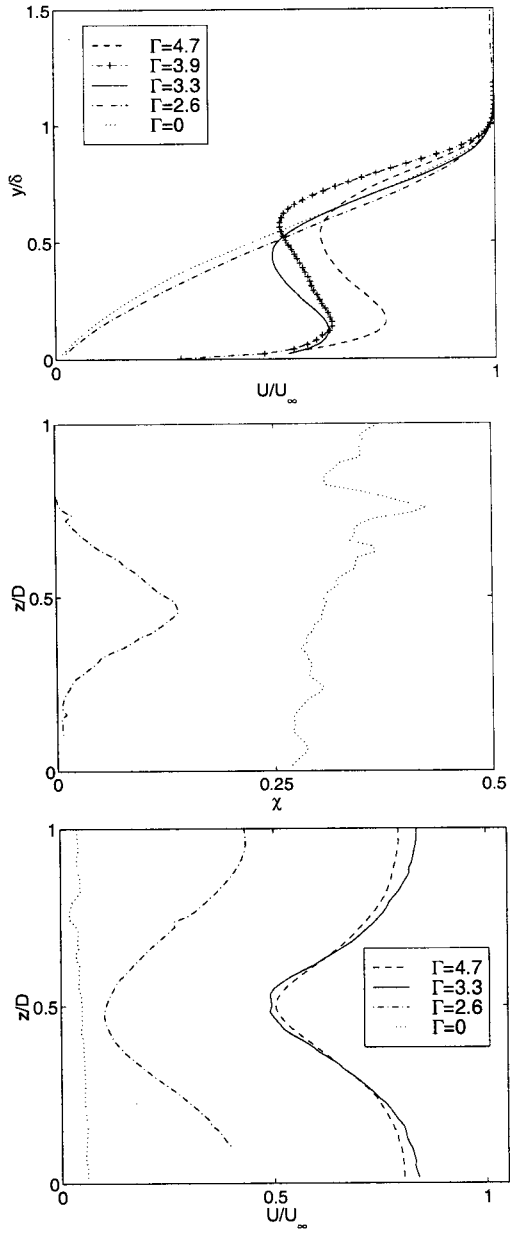

Figure 5: *(a) Streamwise mean velocity profiles at x=2.5 m in the wall-normal direction at the position of outflow (b) the backflow coefficient in the spanwise direction at y=10 mm (c) mean velocity profiles in the spanwise direction at y=10 mm.*

when $x/h \geq 17$, see table 4. Angele and Grewe (2002) found that when $x/h \leq 13$ the vortices are not yet equidistant. It can also be concluded that once the vortices have become equidistant they remain equidistant since the above cases all correspond to different age in terms of x/h, see table 4. This is contradictory to the inviscid theory which predicts that equidistant vortices are pairing with common outflow which leads to a movement of the vortices out of the boundary layer, see Pearcey (1961). A single vortex pair with common outflow was seen to move out from the ZPG boundary layer in the experiment by Mehta and Bradshaw (1988). However, in Pauley and Eaton (1988) the distance between the vortices with common outflow determined whether the vortices would pair and leave the boundary layer or not.

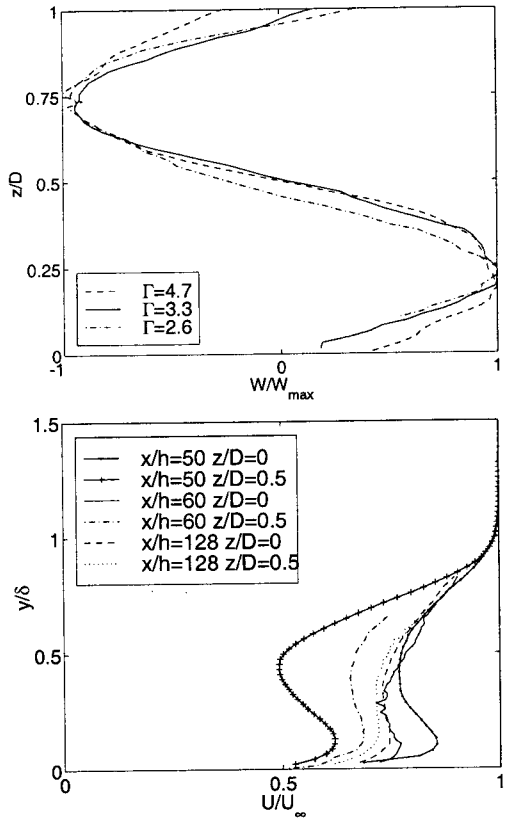

Figure 6: *Mean spanwise velocity profiles at x=2.5 m and the far downstream mean streamwise velocity in the wall-normal direction.*

Asymptotic velocity profile

Angele and Grewe (2002) showed that initially the streamwise mean velocity profile at the position of inflow is extremely full right downstream of a VG. At the position of the vortex center, however, the profile is more strongly S-shaped than the ones observed here in figure 6 (b). Moving downstream this strong three-dimensionality is smeared out and at $x/h \geq 30$ the strong three-dimensionality in τ_w had vanished. The present measurements, displayed in figure 6 (b), show the far downstream behavior. It can be seen that as x/h increase the two profiles at the different spanwise positions of inflow and outflow approach each other. This suggests that the asymptotic state is a two-dimensional boundary layer with S-shaped mean velocity profiles. However, at x/h=128 the vortices are still detectable with weak positive and negative wall-normal velocity respectively which constitutes further evidence of the fact that the vortices are confined to the boundary layer.

VG design

If two cases with different VG height, positioned at different streamwise positions, give a similar circulation, the mean velocity profiles at downstream positions will be similar. The exact profile S-shape depends on the age of the vortices x/h and the initial relative height of the VG, h/δ. This suggests that it is not a crucial matter where the circulation is introduced and how large the vortex is, as long as the circulation is sufficient. This is an effect of the fact that the vortices, and thereby their circulation, is confined to the boundary layer and the circulation is conserved. This is contradictory to the conclusion by Lin *et al* (1989) who

claim that small VGs are more sensitive to their relative position to the separation line. However, all the VGs are relatively large in the present experiment. The chosen VG height and streamwise position, on the other hand, are of importance since they determine the local boundary layer layer parameters U_∞, H_{12} and h/δ which determines the circulation.

The results from the above measurements show that the cases with $\Gamma \geq 3.3$ are all sufficient for backflow elimination in the present case of a weak separation. Using these results suggest that using many relatively small VGs early: n=36, $h/\delta \approx 0.1$, h=2 mm at x=1.1 m, which would give Γ=3.2 would probably be sufficient whereas using few relatively large VGs further downstream n=1.5, $h/\delta \approx 1$, h=60 mm at x=2.0 m, which gives Γ=1.8 would not be sufficient in this specific case. This elucidates the fact that the available Γ decrease in an APG since U_∞ is decreasing and the boundary layer thickness is growing (faster than in a ZPG case) at the same time as the momentum is lost as H_{12} increases. In other words one has to make use of the high momentum available at an early stage.

Small VGs are preferred over large also in terms of penalty drag. The penalty drag induced by the VGs (when c_p, *i.e.* U_∞, is unchanged as in the present case) is estimated as being proportional to the integrated wall shear-stress on the flat plate in downstream direction (which is increased by the vortices) and also as being proportional to the form drag of the VGs. The latter is proportional to the VG size which is why submerged VGs have attracted a lot of attention recently, see for example Lin *et al* (1989). However, small VGs have to be placed far upstream which increase the distance over which the wall shear-stress is increased. This indicates that they should be placed as far downstream as possible. What is optimal depends on the relative size of the two drag contributions. However, the uncontrolled case here is in itself optimal in the sense above *i.e.* $c_f \approx 0$, which minimize the drag induced by the integrated wall shear-stress on the plate. For example the case of Γ=2.6 was shown to lock the backflow into pockets, which is probably decreasing the three-dimensionality of the separation and make the risk of flapping and pressure fluctuations smaller. In a general case the optimal VG streamwise position in terms of induced drag and the specific value of the circulation which is needed depends on the shape of the pressure gradient which governs the downstream development of U_∞, H_{12}, δ and χ.

ACKNOWLEDGMENTS

Special thanks to my supervisor Barbro Muhammad-Klingmann and Marcus and Ulf for great help in the workshop. This project was founded by The science research councel. Special thanks to my friend F. Grewe at the HFI, who spent a week in Stockholm during some of the xz-plane measurements.

REFERENCES

Angele K., and Grewe F., 2002, "Streamwise vortices in turbulent boundary layer separation control", *Submitted to Experiments in Fluids*

Lin J., and Howard F., and Selby G., 1989, "Turbulent flow separation control through passive techniques", *AIAA PAPER 89-0976*

Mehta R. D., and Bradshaw P., 1988, "Longitudinal vortices imbedded in turbulent boundary layers Part 2. Vortex pair with common flow upwards", *J. Fluid Mech.*, Vol. 188, pp. 529-546

Pauley and Eaton J., 1988, "Experimental study of the development of longitudinal vortex pairs embedded in a turbulent boundary layer", *AIAA J.*, vol. 26, no. 7, pp. 816-823

Pearcey H. H., 1961, "Shock-induced separation and its prevention by design and boundary-layer control", in "Boundary Layer and Flow Control, its Principle and Applications", Vol 2, Edited by G. V. Lachmann pp. 1166-1344, Pergamon press, Oxford, England

Schubauer G., and Spangenberg W., 1960 "Forced mixing in boundary layers", *J. Fluid Mech.*, Vol. 8, pp. 10-32.